The American Journal of Pathology, Vol. 189, No. 8, August 2019

The American Journal of
PATHOLOGY
ajp.amjpathol.org

NEUROBIOLOGY

Apolipoprotein E/Amyloid-β Complex Accumulates in Alzheimer Disease Cortical Synapses via Apolipoprotein E Receptors and Is Enhanced by *APOE4*

Tina Bilousova,[*†‡] Mikhail Melnik,[*†] Emily Miyoshi,[*] Bianca L. Gonzalez,[*] Wayne W. Poon,[§] Harry V. Vinters,[‡¶] Carol A. Miller,[‖] Maria M. Corrada,[§**] Claudia Kawas,[§**††] Asa Hatami,[§‡‡] Ricardo Albay, III,[§‡‡] Charles Glabe,[§‡‡] and Karen H. Gylys[*†]

From the University of California, Los Angeles School of Nursing, the Mary S. Easton Center for Alzheimer's Research at University of California, Los Angeles,† and the Departments of Neurology‡ and Pathology and Laboratory Medicine,¶ University of California, Los Angeles School of Medicine, Los Angeles; the Institute for Memory Impairments and Neurological Disorders,§ and the Departments of Neurology,** Neurobiology and Behavior,†† and Molecular Biology and Biochemistry,‡‡ UC Irvine, Irvine; and the the Departments of Pathology, Neurology, and Program in Neuroscience,‖ Keck University of Southern California School of Medicine, Los Angeles, California*

Accepted for publication
April 11, 2019.

Address correspondence to
Karen H. Gylys, Ph.D., UCLA
School of Nursing, Box 956919
Factor Bldg., Los Angeles, CA
90095-6919. E-mail: kgylys@
sonnet.ucla.edu.

Apolipoprotein E (apoE) colocalizes with amyloid-β (Aβ) in Alzheimer disease (AD) plaques and in synapses, and evidence suggests that direct interactions between apoE and Aβ are important for apoE's effects in AD. The present work examines the hypothesis that apoE receptors mediate uptake of apoE/Aβ complex into synaptic terminals. Western blot analysis shows multiple SDS-stable assemblies in synaptosomes from human AD cortex; apoE/Aβ complex was markedly increased in AD compared with aged control samples. Complex formation between apoE and Aβ was confirmed by coimmunoprecipitation experiments. The apoE receptors low-density lipoprotein receptor (LDLR) and LDLR-related protein 1 (LRP1) were quantified in synaptosomes using flow cytometry, revealing up-regulation of LRP1 in early- and late-stage AD. Dual-labeling flow cytometry analysis of LRP1- and LDLR positives indicate most (approximately 65%) of LDLR and LRP1 is associated with postsynaptic density-95 (PSD-95)—positive synaptosomes, indicating that remaining LRP1 and LDLR receptors are exclusively presynaptic. Flow cytometry analysis of Nile red labeling revealed a reduction in cholesterol esters in AD synaptosomes. Dual-labeling experiments showed apoE and Aβ concentration into LDLR and LRP1-positive synaptosomes, along with free and esterified cholesterol. Synaptic Aβ was increased by apoE4 in control and AD samples. These results are consistent with uptake of apoE/Aβ complex and associated lipids into synaptic terminals, with subsequent Aβ clearance in control synapses and accumulation in AD synapses. *(Am J Pathol 2019, 189: 1621—1636; https://doi.org/10.1016/j.ajpath.2019.04.010)*

Apolipoprotein E4 (*APOE4*) is the major genetic risk factor for late-onset Alzheimer disease (AD), and early observations that apoE colocalizes with plaque amyloid-β (Aβ) in human AD and in mouse models resulted in designation of apoE as a pathologic chaperone that facilitates Aβ deposition.[1,2] However, *APOE* effects on AD pathophysiology are multifactorial, and some are independent of Aβ, including effects on tau pathology, plasticity, neuroinflammation, lipid metabolism, mitochondrial function, and blood-brain barrier.[3] In addition to colocalization in plaques,[2,4] apoE and Aβ also colocalize in brain parenchyma from aged

Supported by NIH grants AG27465 (K.H.G.), AG051946 (K.H.G.) and AG18879 (C.A.M.). H.V.V. is supported by the Daljit S. and Elaine Sarkaria Chair in Diagnostic Medicine. Tissue was obtained from the AD Research Center Neuropathology Cores of University of Southern California National Institute on Aging (NIA) grant P50 AG05142, University of California, Los Angeles NIA grant P50 AG 16970, and UC Irvine NIA grant P50 AG16573. Flow cytometry was performed in the University of California, Los Angeles Jonsson Comprehensive Cancer Center (JCCC). The Center for AIDS Research Flow Cytometry Core Facility was supported by NIH grants CA16042 and AI 28697, the JCCC, the University of California, Los Angeles AIDS Institute, the David Geffen School of Medicine, and the Chancellor's Office at University of California, Los Angeles. Diagnosis, characterization, and follow-up of >90 study subjects was supported by NIA grant R01AG21055 (M.M.C., C.K.).

Disclosures: None declared.

https://doi.org/10.1016/j.ajpath.2019.04.010

PDAPP/TRE4 mice, a mouse model of AD named for the platelet derived growth factor (PD) driven production of amyloid precursor protein (APP) with targeted replacement of mouse apoE with human apoE4 (TRE4).[5] ApoE and Aβ colocalize in cortical synaptic terminals in aged control, AD, and aged TRE samples.[6] In this work, apoE 2/4 synapses showed the highest levels of apoE and the lowest levels of Aβ compared with apoE 3/3 and 4/4 terminals, consistent with literature that implicates an apoE isoform in Aβ clearance pathways.[7–11]

Uptake by the apoE receptors, low-density lipoprotein receptor (LDLR) and LDLR-related protein 1 (LRP1), makes an important contribution to Aβ clearance, and in the brain these pathways operate in neurons, brain microvasculature, astrocytes, and microglia.[12] For example, overexpression of LDLR reduces Aβ deposition without affecting amyloid precursor protein expression in multiple mouse strains,[13] and reduction of neuronal LRP1 in amyloid precursor protein/presenilin 1 (PS1) mice increases brain Aβ deposition.[14] On the other hand, receptor-mediated clearance of Aβ into neurons may lead to toxic accumulations,[15,16] whereas internalization by microglia,[17] endothelial cells,[9] or astrocytes[18] seems a more likely pathway for uptake and degradation of Aβ.[19]

ApoE/Aβ complexes have been detected in human brain extracts,[20] plasma,[21] and cerebral spinal fluid,[22] and some key Aβ-dependent apoE effects on AD seem likely to result from direct interactions between apoE and Aβ. However, the variability arising from multiple detection methods has greatly limited understanding of the role of complex formation in disease progression, as documented in recent reviews.[12,23] An additional level of variability emerges from the disparate factors that affect binding of apoE to Aβ; these include apoE isoform, apoE lipidation state, and aggregation state of Aβ.[12,23] A reduction in detectable complex with apoE4 has led to one hypothesis that apoE/Aβ complex level modulates Aβ levels and that reduced lipidation of apoE results in reduced complex formation and increased Aβ accumulation.[23,24] Lipidation status is difficult to assess *in vivo*, but apoE4 is generally believed to be less lipidated than apoE3. This hypothesis is supported by experiments in mice expressing five familial AD mutations (5XFAD) plus human apoE isoforms[23] and also by recent data showing that apoE4 reduces lipidation and enhances Aβ accumulation, whereas apoE2 has the opposite effect.[25] However, several studies demonstrate that blocking the apoE/Aβ interaction reduces Aβ deposition,[26–28] contradicting the role of the complexes in Aβ clearance and suggesting important therapeutic implications of apoE/Aβ complex formation.

Given the promise of *APOE*-related therapeutics for increasing clearance or reducing accumulation of Aβ,[3,19] it is critical to understand the pathway(s) affected by interactions between apoE and Aβ. On the basis of previous data suggesting that apoE isoform affects apoE/Aβ complexes and Aβ clearance, and on our previous work showing that apoE enhances uptake of Aβ into synaptosomes,[29] the present studies examined the hypothesis that apoE receptors mediate uptake of apoE/Aβ complex and lipids into the synaptic compartment in cortical synapses of aged control and AD samples. Multiple SDS-stable apoE/Aβ complexes were observed in human cortical synaptosomes, and complex level was increased in AD samples. Using flow cytometry analysis, we also demonstrate alterations in synaptic lipids and pronounced accumulation of both apoE and Aβ in LRP1- and LDLR-positive synaptosomes, consistent with uptake of Aβ and apoE into the synaptic compartment by these receptors. Experiments also showed that higher synaptic Aβ was associated with apoE4.

Materials and Methods

Materials

The antibodies used in the present work are detailed in Table 1.[30,31] The dyes filipin and Nile red [5H-benzo(a) phenoxazin-5-one, 9-(diethylamino)-7385-67-3] were purchased from Sigma-Aldrich (St. Louis, MO).

Human Brain Specimens

Brain samples of parietal cortex (Brodmann areas A7, A39, and A40) were obtained at autopsy from Alzheimer disease research centers at University of California, Los Angeles, University of California, Irvine, and University of Southern California (Table 2). Samples were selected for each experiment on the basis of the design and availability in the bank, and neurologic controls were used interchangeably with the aged cognitively normal controls. Table 2 lists the total of unique cases (28 controls, 80 AD); some cases were used for more than one experiment. As in a recent study,[32] cases were stratified into early (Braak stages II–IV) and late (Braak stages V and VI) AD on the basis of Braak stage because of the inherent dynamic range and long general use of this staging system. Immediately on receipt, samples (approximately 0.3 to 5 g) were minced in a 0.32 mol/L sucrose solution with protease inhibitors for cryopreservation of synaptic structure and membranes[33] (2 mmol/L EDTA, 2 mmol/L EGTA, 0.2 mmol/L phenylmethylsulfonyl fluoride, 1 mmol/L Na pyrophosphate, 5 mmol/L NaF, and 10 mmol/L Tris), then stored at −70°C until homogenization. The P-2 (crude synaptosome; synaptosome-enriched fraction) was prepared as previously described[29]; briefly, tissue was homogenized in ice-cold buffer [0.32 mol/L sucrose; 10 mmol/L Tris, pH 7.5; plus protease inhibitors pepstatin (4 μg/mL), aprotinin (5 μg/mL), trypsin inhibitor (20 μg/mL), EDTA (2 mmol/L), EGTA (2 mmol/L), phenylmethylsulfonyl fluoride (0.2 mmol/L), and Leu-peptin (4 μg/mL)]. The homogenate was first centrifuged at 1000 × *g* for 10 minutes; the resulting supernatant was centrifuged at 10,000 × *g* for 20 minutes to obtain the crude synaptosomal pellet. Aliquots of P-2 are routinely cryopreserved in 0.32 mol/L sucrose and banked at −70°C until the day of the

Table 1 Reagents

Antibody	Antigen/epitope	Supplier	Host	Reactivity
10G4	Aβ peptide: N-terminal residues 5 to 17	Kind gift of Greg Cole (Veterans Affairs Medical Center; University of California)[30]	Mouse	Human, mouse
6E10	N-terminal residues 1 to 16 of Aβ peptide	BioLegend (San Diego, CA)	Mouse	Human
mOC1	Fibrillar aggregates of amyloid-β	Kind gift of Charles Glabe (University of California)[31]	Rabbit	Human
mOC16	Fibrillar aggregates of amyloid-β	Kind gift of Charles Glabe[31]	Rabbit	Human
mOC23	Fibrillar aggregates of amyloid-β	Kind gift of Charles Glabe[31]	Rabbit	Human
mOC98	Fibrillar aggregates of amyloid-β	Kind gift of Charles Glabe[31]	Rabbit	Human
Anti—PSD-95 antibody	PSD-95	Millipore (Temecula, CA)	Mouse	Human
Synaptophysin antibody	Synaptophysin	Gene Tex (Irvine, CA)	Rabbit	Human, mouse, rat
SNAP-25 antibody (SP12) sc-20038	SNAP-25	Santa Cruz Biotechnology (Dallas, TX)	Mouse	Human, mouse
Anti-apoE goat pAb (178479)	ApoE	Calbiochem (Cambridge, MA)	Goat	Human, mouse, rat
E6D7	ApoE	Abcam (Cambridge, MA)	Mouse	Human, mouse
EP1553Y	LDLR	Abcam	Rabbit	Human, mouse
EPR3724	LRP1	Abcam	Rabbit	Human, mouse, rat, pig
Filipin (dye)	Free cholesterol	Sigma-Aldrich (St. Louis, MO)	NA	NA
Nile red (dye)	Cholesterol esters	Sigma-Aldrich	NA	NA

ApoE, apolipoprotein E; NA, not applicable; mOC, OC monoclonal; pAb, polyclonal antibody; postsynaptic density-95, PSD-95; SNAP-25, synaptosomal nerve-associated protein 25.

experiment,[33] at which time they were defrosted at 37°C, resuspended in phosphate-buffered saline (PBS) with protease inhibitors, sonicated, and centrifuged for 4 minutes at 3380 × *g*. Supernatant was collected, and total protein concentration was defined using the bicinchoninic acid protein assay (Pierce, Waltham, MA).

Western Blot and Dot Blot Analysis

Human P-2 samples were separated by nonreducing gel electrophoresis on 10% to 20% Tris-glycine gradient gels either with or without reducing agent dithiothreitol. After transferring to Immobilon-P membrane (Millipore, Burlington, MA), Western blot analysis with primary anti-apoE (E6D7) or anti-Aβ primary antibody (10G4 or 6E10) and secondary anti-mouse horseradish peroxidase—conjugated IgG (Jackson Immunoresearch, West Grove, PA) was performed. Before immunolabeling, membranes were labeled with Ponceau S (0.1% w/v in acetic acid) to verify equal loading; only membranes with equal loading were used for analysis. Immunolabeled proteins were visualized by SuperSignal West Femto maximum sensitivity substrate (Thermo Scientific, Rockford, IL). Resulting films were scanned and quantified on a UVP 600 imaging system (BioSpectrum, Jena, Germany) using VisionWorks software version 6.6A (VisionWorks, Upland, CA). For dot blotting, 1 μL of each sample was pipetted onto a Whatman nitrocellulose membrane (GE Healthcare, Chicago, IL). Membranes were allowed to air dry and were subsequently blocked in 10% nonfat dry milk in Tris-buffered saline (TBS) containing 0.01% Tween 20 (TBS-T) for 1 hour at room temperature. Membranes were then incubated 1:100 with OC monoclonal (mOC) antibodies in 5% nonfat dried milk in TBS-T overnight

Table 2 Case Information for Human Samples

Variable	Aged controls*	Neurologic controls†	Early AD (Braak stage ≤ IV)	Late AD (Braak stage V or VI)
Cases, *n*	21	7	23	57
Age, y‡	85.3 ± 7.3	66.5 ± 7.3	85 ± 8.9	81.2 ± 12.3
PMI, hours‡	6.9 ± 3.7	8.1 ± 4.5	7.6 ± 3.0	6.2 ± 2.0
Female sex, %	48	75	57	38
APOE4 positive, *n*	5	2	8	28

*No dementia.
†Without AD pathology (spinocerebellar ataxia, Pick disease, vascular dementia, and Parkinson disease with dementia).
‡Data are given as means ± SD.
PMI, post-mortem interval.

at 4°C. After three 5-minute washes in TBS-T, membranes were incubated with horseradish peroxidase—conjugated goat anti-rabbit IgG (1:10,000 in 5% nonfat dried milk in TBS-T). Membranes were then washed three times for 5 minutes in TBS-T and visualized using enhanced chemiluminescence (GE Healthcare). Images were obtained using a Nikon D700 (Nikon Inc., Melville, NY) camera, as described previously.[31]

Immunoprecipitation

Antibodies were covalently coupled to M-270 Epoxi Dynabeads using a conjugation kit (14311D; Invitrogen, Carlsbad, CA), according to manufacturer's instructions. P-2 samples were quickly thawed, centrifuged at 10,000 × *g* for 10 minutes at 4°C to remove sucrose, homogenized in PBS with protease and phosphatase inhibitor cocktail (Thermo Scientific; v/w 1:9) using a pestle motor mixer (30 seconds on ice), and then run through three freeze-thaw cycles (3 minutes liquid nitrogen, 30 minutes thawing at room temperature) with additional 30 seconds' homogenization after each cycle. Samples were centrifuged at 840 × *g* for 2 minutes at 4°C, and supernatants (P2-H) were collected. Small volumes of each P2-H sample were set aside for further Western blot analysis; the rest were equally divided for immunoprecipitation (IP) with E6D7, 6E10, and corresponding isotype control antibody conjugated Dynabeads. Specificity for the E6D7 antibody has been demonstrated in apoE knockout mice.[34] Samples were rotated with the beads for 1 hour at 4°C, then placed on magnet, and unbound flow throughs were collected; beads were washed three times with PBS using magnet. P2-H, flow-through samples, and beads were mixed with Tris-glycine sample buffer with DDT and boiled for 10 minutes. Beads were placed on magnet, and the fractions containing apoE/Aβ complexes (IP) were collected. Samples were run using 10% to 20% Tris-glycine SDS-PAGE gel and transferred to polyvinylidene difluoride membrane. Membranes were blocked with 3% milk and 5% bovine serum albumin for 1 hour at room temperature and probed with either goat anti-apoE (178479; Calbiochem, Cambridge, MA) or mouse anti-Aβ antibodies (BioLegend, San Diego, CA) at 4°C. After washes, membranes were incubated with corresponding horseradish peroxidase—conjugated secondary antibodies for 1 hour at room temperature, SuperSignal West Femto maximum sensitivity substrate was applied for 5 minutes, and images were taken using a UVP reading system (BioSpectrum).

Immunolabeling and Lipid Dye Labeling

P-2 fractions were prepared from cryopreserved brain tissue, as described previously[35]; cryopreserved in 0.32 mol/L buffered sucrose solution; and stored at −80°C as aliquots. On the day of the experiment, aliquots were quickly defrosted at 37°C and P-2 pellets were collected by centrifugation. After fixation in 0.25% paraformaldehyde/PBS (1 hour at 4°C), and permeabilization in 0.2% Tween 20/PBS solution (15 minutes at 37°C), the pellets were incubated with Aβ, apoE, synaptophysin (SYP), synaptosomal nerve-associated protein 25, PSD-95, LDLR, or LRP1-specific antibodies and directly labeled with Alexa 488 or Alexa 647 fluorochromes using Zenon isotype-specific labeling kits (Thermo Fisher; 30 minutes at room temperature). Immunolabeled P-2 pellets were washed with 0.2% Tween 20/PBS and resuspended in 500 μL of PBS for flow cytometry analysis. Stock solutions were prepared as 1 mg/mL solutions and stored in −20°C protected from light; Nile red stock was made in dimethyl sulfoxide, and filipin stock was prepared in 95% ethanol. On the day of the experiments, the stock solutions were diluted 1:1000 in Tris—hydrochloric acid, and 100 μL of this mixture was incubated with P-2 aliquots for 30 minutes at room temperature, protected from light.

Image Stream Analysis

Synaptosome imaging was done in an ImageStream MarkII multispectral imaging flow cytometer fitted with a 60× microscope objective (Amnis Corp., Seattle, WA). A total of 25,000 events were collected per sample. IDEAS software version 6.1 (Luminex, Austin, TX) was used for analyzing raw images. A compensation matrix was applied to all of the data.

Flow Cytometry Analysis

Data were acquired using a BD-FACS Calibur analytical flow cytometer (Becton-Dickinson, San Jose, CA), equipped with argon 488-nm, helium-neon 635-nm, and helium-cadmium 325-nm lasers. Debris was excluded by establishing a size threshold set on forward light scatter. A total of 10,000 particles were collected and analyzed for each sample; an additional 2000 Aβ-, LDLR-, LRP1-, SYP-, or PSD-95—positive particles were collected for experiments investigating corresponding subpopulations of synaptosomes. Alexa 488 and Alexa 647 were detected by FL-1 and FL-4 channel photomultiplier tubes, respectively. Analysis was performed using FCS Express software version 3 (DeNovo Software, Waterloo, ON, Canada). Statistical comparisons used *t*-test unless otherwise noted, and error bars represent SEM.

Results

SDS-Stable ApoE/Aβ Complex Is Markedly Increased in AD Compared with Control Synaptosomes

Using different methods that include the appearance of complex on Western blot analyses, several articles have documented formation of SDS-stable apoE/Aβ complex *in vitro*.[36–40] We have also used co—enzyme-linked immunosorbent assay to demonstrate isoform-mediated changes in levels of soluble apoE/Aβ complex.[24] Initial experiments (Figure 1, A and B) used side-by-side Western

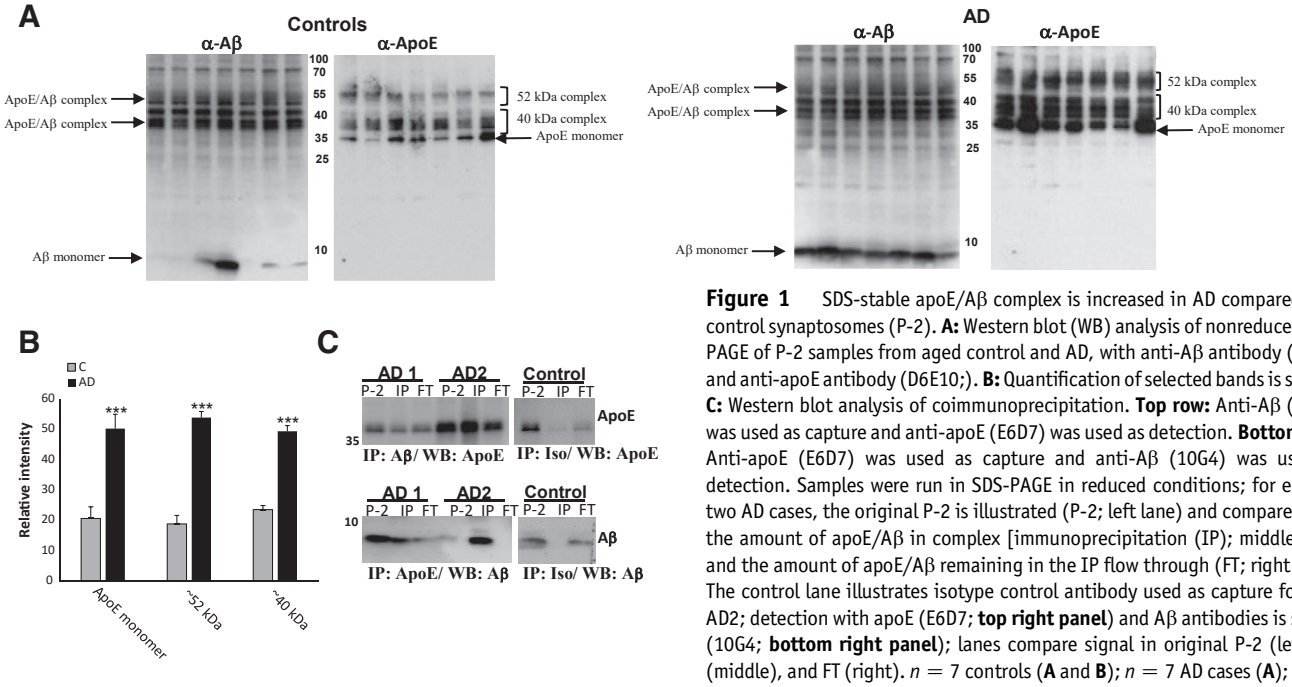

Figure 1 SDS-stable apoE/Aβ complex is increased in AD compared with control synaptosomes (P-2). **A:** Western blot (WB) analysis of nonreduced SDS-PAGE of P-2 samples from aged control and AD, with anti-Aβ antibody (10G4) and anti-apoE antibody (D6E10;). **B:** Quantification of selected bands is shown. **C:** Western blot analysis of coimmunoprecipitation. **Top row:** Anti-Aβ (10G4) was used as capture and anti-apoE (E6D7) was used as detection. **Bottom row:** Anti-apoE (E6D7) was used as capture and anti-Aβ (10G4) was used as detection. Samples were run in SDS-PAGE in reduced conditions; for each of two AD cases, the original P-2 is illustrated (P-2; left lane) and compared with the amount of apoE/Aβ in complex [immunoprecipitation (IP); middle lane] and the amount of apoE/Aβ remaining in the IP flow through (FT; right lane). The control lane illustrates isotype control antibody used as capture for case AD2; detection with apoE (E6D7; **top right panel**) and Aβ antibodies is shown (10G4; **bottom right panel**); lanes compare signal in original P-2 (left), IP (middle), and FT (right). $n = 7$ controls (**A** and **B**); $n = 7$ AD cases (**A**); $n = 8$ AD cases (**B**). $^{***}P < 0.001$ versus control (C).

blot analysis of SDS-PAGE with antibodies against Aβ and apoE. Western blot analysis of P-2 samples revealed monomeric apoE at approximately 35 kDa and monomeric Aβ bands at approximately 8 kDa (Figure 1A), along with a ladder of bands between 35 and 55 kDa. Localization of approximately 40-kDa bands is strictly identical in the Aβ- and apoE-probed Western blot analyses of both control and AD samples and consistent with previously reported SDS-stable apoE/Aβ complexes formed *in vitro*.[39,41] The series of complex bands is approximately the size of a bound SDS-stable Aβ dimer to apoE. Another series of potential complex bands is approximately 52 kDa, approximately the size of a bound SDS-stable tetramer. The laddering pattern likely results from formation of complex with slightly different sizes of Aβ; a ladder of SDS-stable Aβ oligomers is commonly seen by us and others on Aβ Western blot analyses using multiple antibodies.[42–45] The 40- and 52-kDa complex bands with the α-Aβ antibody are similar in controls and AD cases, although they are markedly increased when labeled by the α-apoE antibody E6D7 (Figure 1B). On the basis of our published observations in aged controls,[6] we hypothesize that this result may reflect formation of apoE/Aβ complex in aged control cases as part of nonpathologic clearance versus accumulation intermediates. The higher level of apoE/Aβ complex detected with anti-apoE antibodies may also reflect the binding of other proteins in the complex mixture to Aβ, hindering binding of the Aβ but not the apoE antibody in the AD cases. Quantification of the α-apoE blots showed a marked increase in apoE complex groups and monomeric apoE in AD compared with control synaptosomes, with increases twofold or greater ($P \leq 0.0005$) (Figure 1B).

For direct confirmation of complex formation *in vivo*, a P-2 fraction was prepared from two AD cortex samples (*APOE* 3/4) (Table 1), and coimmunoprecipitation was performed first using anti-apoE as capture (E6D7) and anti-Aβ as detection (mouse; BioLegend) antibody. The reverse strategy was also tested using anti-Aβ antibody (6E10) as capture antibody and anti-apoE antibody (goat polyclonal anti-apoE) as detection antibody (Figure 1C). Immunoprecipitated complex is clear with both α-Aβ and α-apoE antibodies (Figure 1C) for each antibody in each of two AD cases; controls include the original P-2 sample and the flow through. A substantial amount of apoE/Aβ complex is detected in the flow through with the α-apoE antibody, consistent with the results in Figure 1A showing more complex detected with the α-apoE antibody, as discussed above. Precipitation using isotype antibody control in place of anti-apoE and anti-Aβ capture antibodies shows no immunoprecipitation signal (Figure 1C); omission of the primary antibody also showed no signal (data not shown). Taken together, these results demonstrate that a considerable amount of SDS-stable apoE/Aβ complex accumulates within cortical synaptic terminals in AD.

The ApoE Receptor LRP1 Is Up-Regulated in AD Synaptosomes

Confocal and electron microscopy has previously confirmed flow cytometry results and the integrity of synaptosome structures.[46] Imaging flow cytometry is a novel technology that produces an image of each cell/event acquired from a sample. This instrument was used to confirm presynaptic and post-synaptic elements of synaptosomes. Human

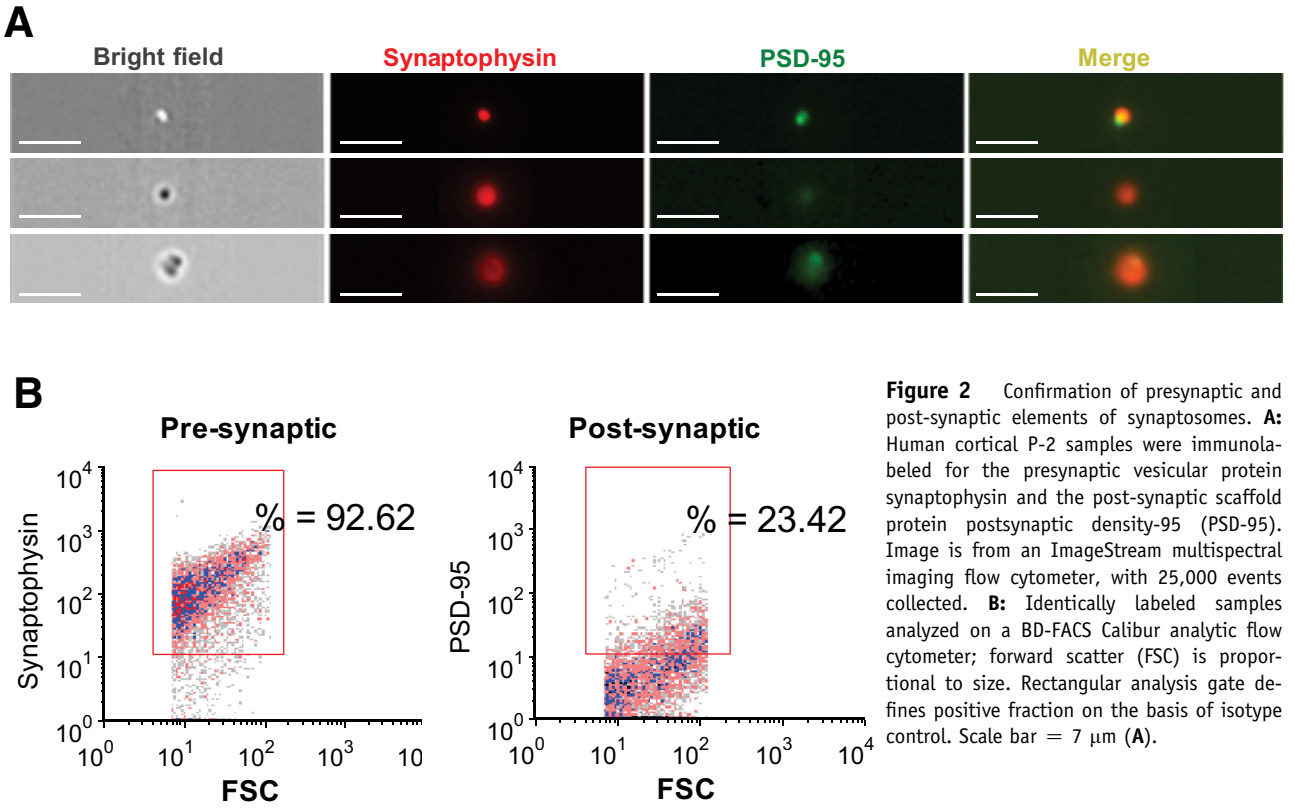

Figure 2 Confirmation of presynaptic and post-synaptic elements of synaptosomes. **A:** Human cortical P-2 samples were immunolabeled for the presynaptic vesicular protein synaptophysin and the post-synaptic scaffold protein postsynaptic density-95 (PSD-95). Image is from an ImageStream multispectral imaging flow cytometer, with 25,000 events collected. **B:** Identically labeled samples analyzed on a BD-FACS Calibur analytic flow cytometer; forward scatter (FSC) is proportional to size. Rectangular analysis gate defines positive fraction on the basis of isotype control. Scale bar = 7 μm (**A**).

cortical P-2 samples were immunolabeled for the presynaptic vesicular protein SYP and the post-synaptic scaffold protein PSD-95, and data were acquired from 25,000 particles. Consistent with previous flow cytometry results, the images (Figure 2A) demonstrated that virtually all of the particles imaged were spherical, were positive for SYP, and had the expected size of approximately 1 μm; equivalent P-2 labeling for three independent presynaptic markers has previously been demonstrated (synaptosomal nerve-associated protein 25, syntaxin, and synaptophysin).[35] Most of the particles demonstrated little to no fluorescent signal for the post-synaptic scaffold protein PSD-95 (Figure 2A), but a subpopulation of particles were labeled for both presynaptic and post-synaptic markers (Figure 2A). Because the instrument has a 60× objective compared with the 100× objective of conventional confocal microscopy, resolution is somewhat reduced. However, a fraction of the dual-labeled population demonstrated a more intact and spherical post-synaptic element (Figure 2A). Overall, the images were in line with our previous characterizations of human cortical synaptosomes, with >90% presynaptic and approximately 20% positive for a post-synaptic element by conventional flow cytometry, as previously published[46] and illustrated by representative dot plots (Figure 2B).

On the basis of the abundance of apoE, Aβ, and apoE/Aβ complex in synaptosomes, two major apoE receptors, LDLR and LRP1, both members of the core LDLR receptor gene family previously shown to have brain apoE and Aβ levels, were next investigated.[19,47] Synaptosomes were immunolabeled with antibodies to each receptor using a protocol for staining of intracellular antigens in which the P-2 is first lightly fixed and then permeabilized. Synapse-associated labeling was quantified using flow cytometry, with data collected from 10,000 particles/sample. The analysis gate was drawn on the basis of size standards and included only particles between 0.75 and 1.5 μm; immunolabeling is plotted against forward scatter, which is proportional to size. Representative plots illustrate the flow cytometry analysis; SYP was used as a positive control (Figure 3A) and illustrates the relative purity of synaptosomes within the analysis size gate (approximately 90% positive). Isotype-specific antibodies were used to determine background labeling (Figure 3B). Representative plots for LRP1 immunolabeling in a control versus AD sample are presented (Figure 3, C and D); as shown in the aggregate data (Figure 3E), LRP1 antibody labels approximately 14% of synaptosomes in controls, which increases to approximately 24% in early AD (Braak stages II to IV; $P < 0.05$) and remains at approximately 24% in late AD (Braak stages V to VI; $P < 0.05$). LDLR also trended upward in both early- and late-stage AD cases, indicating compensatory up-regulation of apoE receptors in AD synapses.

LRP1 and LDLR Receptors Are Not Exclusively Post-Synaptic

Members of the LDLR family are well established as mediators of Aβ uptake and lysosomal trafficking and clearance in

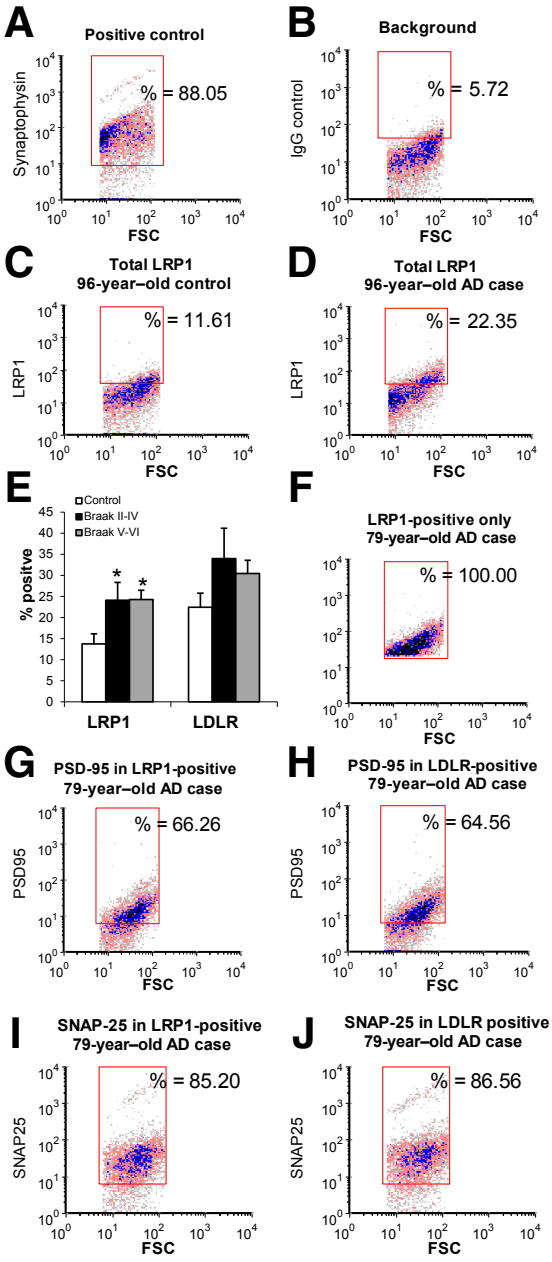

Figure 3 LRP1 is up-regulated in AD compared with control synaptosomes and localized to presynaptic and post-synaptic elements. **A**–**D:** P-2 samples were immunolabeled with antibodies against LDLR and LRP1, then analyzed by flow cytometry; dot plots from representative samples demonstrate typical positive control (**A**) and background in the presence of isotype control antibody (**B**), along with representative immunolabeling for LRP1 in control (**C**) and AD samples (**D**). Fluorescence is plotted against forward scatter (FSC), which is proportional to size. **E:** Aggregate data are shown for receptor-positive fraction. **F** and **G:** Samples were dual labeled for LRP1, LDLR, and postsynaptic density-95 (PSD-95); 2000 particles were collected for each sample. **F**–**H:** Representative samples illustrate collection of LRP1 positives (**F**) and PSD-95 immunofluorescence in LRP1 positives (**G**) and LDLR positives (**H**). **I** and **J:** Representative samples illustrate presynaptic fraction in samples dual labeled for synaptosomal nerve-associated protein 25 (SNAP-25) and LRP1 (**I**) and LDLR (**J**). Rectangular analysis gate defines positive fraction on the basis of isotype control. Data are expressed as means ± SEM (**E**). $n = 5$ controls (**E**); $n = 6$ Braak stages II to IV (**E**); $n = 7$ Braak stages V to VI (**E**). $^*P < 0.05$ versus control.

neurons, glial cells, and vascular endothelial cells.[12,48,49] At the same time, these receptors are known to interact with post-synaptic scaffolding proteins and have well-established roles in signaling,[50–52] leading to a conclusion that LRP1 and LDLR are primarily post-synaptic.[53,54] Therefore, dual-labeling experiments were performed with presynaptic and post-synaptic proteins to investigate the synaptic location of these apoE receptors. Cortical P-2 samples were dual labeled for LDLR or LRP1 and with the N-methyl-D-aspartate receptor scaffold PSD-95; flow cytometry data were collected from the total population (10,000 particles) and from LDLR- and LRP1-positive synaptosomes (2000 particles/sample). When only LRP1 positives were collected, 66% of synaptosomes in a representative dot plot were positive for PSD-95 (Figure 3, F and G); in the aggregate data, the mean was 63% ± 5.6% in controls and 68% ± 3.6% in AD synaptosomes (data not shown). This result suggests that the remaining approximately 35% of LRP1 positives are exclusively presynaptic because our previous work has established that approximately 95% of size-gated particles are synaptosomes.[46,55,56] A parallel experiment with collection of LDLR positives revealed a similar degree of post-synaptic association, with 59% ± 8.0% and 65% ± 7.6% positive for PSD-95 in control (data not shown) and a representative AD sample, respectively (Figure 3H). Similar dual-labeling experiments with each receptor and synaptosomal nerve–associated protein 25, followed by collection of LRP and LDLR positives, confirms the localization of apoE receptors to synaptosomes, with 85% and 87% positive for synaptosomal nerve–associated protein 25, respectively (Figure 3, I and J). Therefore, the two apoE receptors demonstrate both presynaptic and post-synaptic localization in control and in AD cortex. These results confirm previous results showing physical association of most LRP1 and LDLR receptors with post-synaptic scaffold proteins,[51–53,57,58] and they indicate that a smaller population of both receptors is exclusively localized to the presynapse.

Free Cholesterol Is Increased and Esterified Cholesterol Is Reduced in AD Synapses

A good deal of evidence indicates that lipid metabolism modulates Aβ levels, and recently, several genes regulating lipid metabolism have been implicated in AD.[59] Therefore, flow cytometry was used to examine the levels of free and esterified cholesterol in synaptosomes across disease stage (Figure 4). The fluorescent polyene antibiotic filipin was used to label free (unesterified) cholesterol,[60,61] and the dye Nile red was used to label esterified cholesterol [cholesterol esters (CEs) and lipid droplets[62]]. Representative dot plots for the analysis are shown in Figure 4, A–C; an unstained CE blank sample is shown (Figure 4A), along with representative synaptosome labeling from a control case for CE (Figure 4B) and for free cholesterol (Figure 4C). IgG-labeled control samples are not needed because lipid labels are dyes rather than antibodies. As expected, virtually

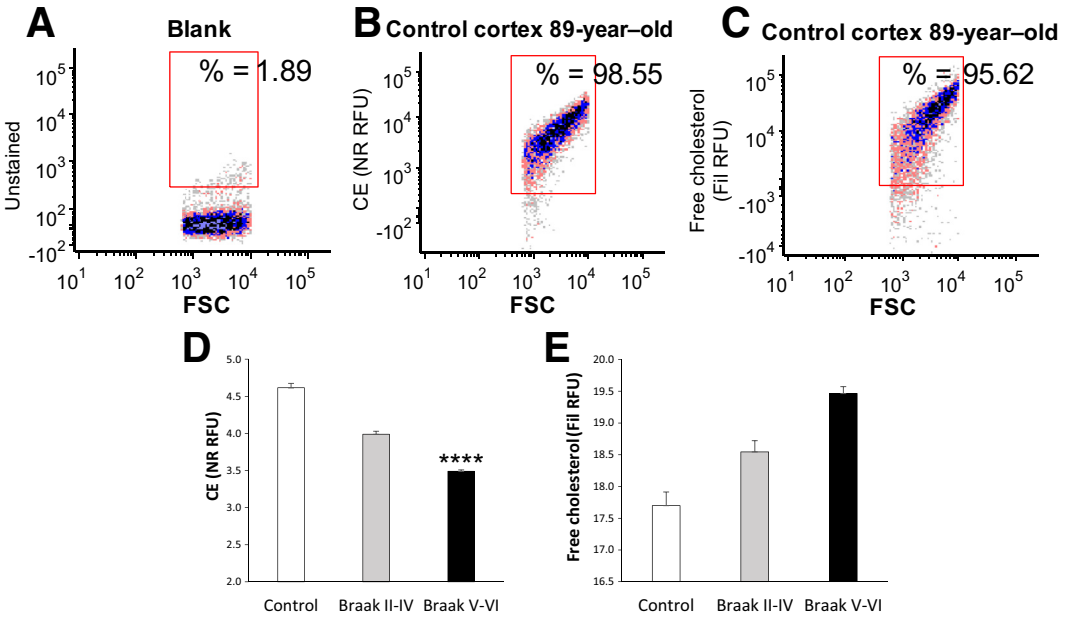

Figure 4 Esterified cholesterol is reduced in AD compared with control synaptosomes. **A**–**C:** Representative samples illustrate flow cytometry analysis of lipid labeling in cortical synaptosomes (**A**), background (**B**), Nile red (NR) [cholesterol esters (CEs)], and filipin (Fil) (free cholesterol; **C**). Fluorescence is plotted against forward scatter (FSC), which is proportional to size, and 5000 particles were collected for each sample. **D** and **E:** Aggregate data are shown for cholesterol esters (**D**) and free cholesterol (**E**); relative fluorescence unit (RFU) is plotted as thousands. Rectangular analysis gate defines positive fraction on the basis of blank control. Data are expressed as means ± SEM (**D** and **E**). $n = 13$ controls (**D** and **E**); $n = 11$ Braak stages II to IV (**D** and **E**); $n = 28$ Braak stages V and VI (**D** and **E**). ****$P < 0.0001$ versus control (one-way analysis of variance).

all synaptosomes are brightly positive for both lipid dyes. The aggregate data demonstrate that CE levels, presented as relative fluorescence units, are lower in AD compared with control synapses, with a progressive reduction observed across disease stage [$F(2,48) = 9.41$; $P < 0.001$] (Figure 4D). The opposite trend is seen for free cholesterol, where cholesterol shows progressive elevation with disease stage (Figure 4E). This experiment used more samples (11 to 28 per group) to add power for detection of *APOE*-mediated differences; however, no consistent lipid changes were associated with *APOE* genotype (data not shown). These results demonstrate that AD alters cholesterol homeostasis in synaptic terminals, suggestive of reduced cholesterol stores late in disease.

ApoE and Aβ Are Concentrated into LDLR- and LRP1-Positive Synapses

On the basis of the high levels of SDS-stable apoE/Aβ complex in synaptosomes and our previous demonstration that Aβ is concentrated in apoE-positive synapses in both human and rodent cortex,[6] we hypothesized that apoE/Aβ complex enters terminals via apoE receptors. Parietal cortex samples from aged control samples were dual labeled for apoE and for LDLR or LRP1; flow cytometry data were collected from the total population (10,000 particles) and from LDLR- and LRP1-positive synaptosomes (5000 particles/sample), to compare the apoE level in the total population with the level of apoE in synapses positive for apoE receptors. The analytic strategy is illustrated by the representative dot plots of the same sample in Figure 5, A–C: Figure 5A shows apoE level in the total population of synaptosomes (14.19%), Figure 5B illustrates the acquisition of synaptosomes that are exclusively LDLR positive (100%), and Figure 5C illustrates the enormous enrichment of apoE in the LDLR-positive terminals (95.48%). A parallel experiment quantified Aβ in receptor-positive synapses; the aggregate data are shown for apoE in Figure 5D and for Aβ in Figure 5E. In control samples, the apoE antibody labeled 21% of the total synaptosome population, and this increased to 91% ($P < 0.0001$) in LRP1-positive synapses and 91% in LDLR-positive synapses ($P < 0.0001$), indicating a striking accumulation of apoE into synaptosomes by both receptors. The apoE-positive fraction of synaptosomes increased from 21% in control samples to 32% in AD ($P < 0.03$) (Figure 5D), consistent with previous flow cytometry results.[6] In AD samples, accumulation of apoE in receptor-positive synaptosomes was almost identical to that seen in aged controls, increasing from 32% to 96% ($P < 0.0001$) and to 93% ($P < 0.0001$), for LRP1 and LDLR positives, respectively (Figure 5D). These results suggest that both LDLR and LRP1 receptors mediate apoE uptake into synaptic terminals, and that receptor-mediated uptake of apoE and Aβ into terminals occurs in both control and AD synapses.

The parallel experiment with dual labeling for Aβ (10G4 antibody) with either LDLR or LRP1 demonstrated similar results (Figure 5E). Aβ increased in the total synaptosome

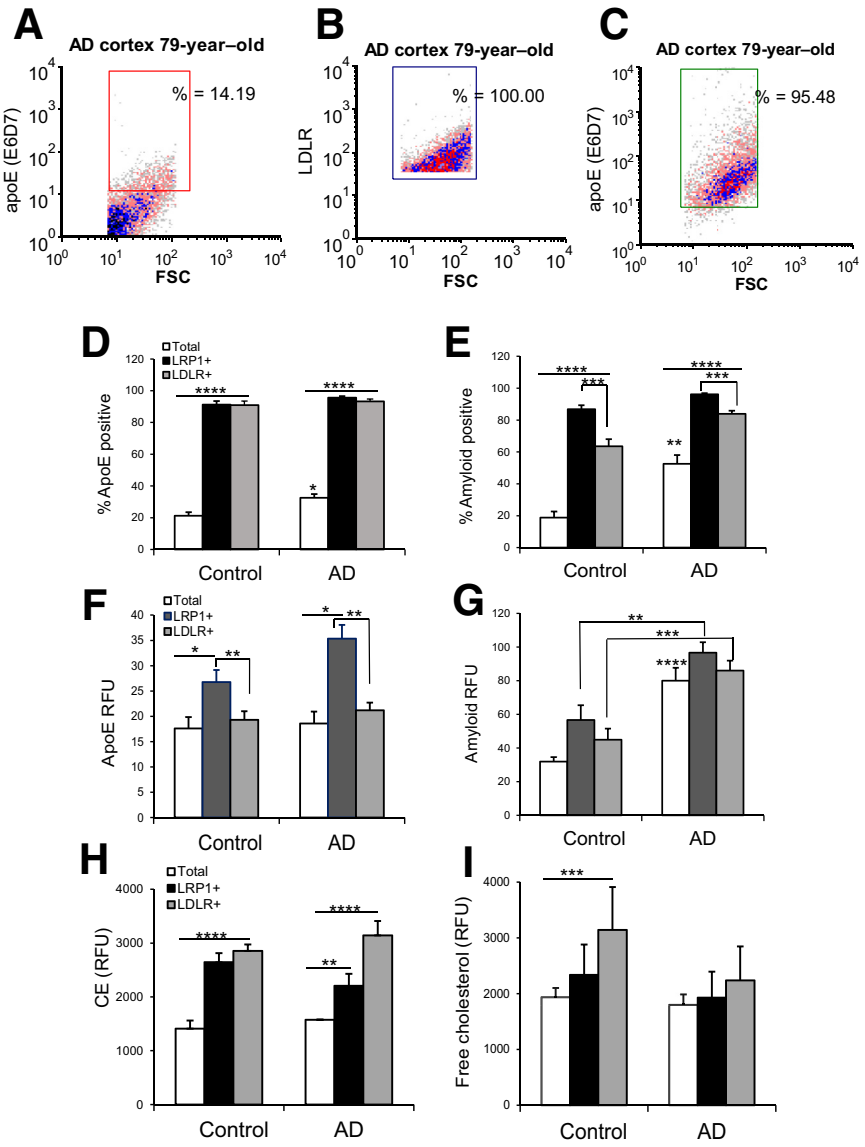

Figure 5 ApoE and Aβ colocalization with LRP1 and LDLR in individual synaptosomes from AD cortex. **A**–**C:** The analytic strategy is illustrated by a representative sample dual labeled for apoE and LDLR. Fluorescence is plotted against forward scatter (FSC), which is proportional to size, and 2000 particles were collected for each sample. Dot plots illustrate the size of the apoE-positive fraction in the total population of cortical synaptosomes (**A**), the collection of receptor-positive synaptosomes for the same sample (**B**), and the enrichment of apoE in LDLR positives (**C**). **D**–**G:** Aggregate data show the labeling of apoE in LRP and LDLR positives for control and AD samples. **D** and **E:** Size of the positive fraction. **F** and **G:** Relative fluorescence unit (RFU) parameter, which indicates per-terminal brightness of immunolabeling. **H** and **I:** Lipid levels in apoE-receptor positives using the same analytic strategy as above. The level of cholesterol esters (CEs) in receptor positives is shown (Nile red; **H**), and the level of free cholesterol (labeled by filipin) is shown (**I**). Rectangular analysis gate defines positive fraction on the basis of isotype control. $n = 6$ control samples (**D**–**I**); $n = 5$ AD samples (**D**–**I**). $^{*}P < 0.05$, $^{**}P < 0.01$, $^{***}P < 0.001$, and $^{****}P < 0.0001$ versus control, unless otherwise indicated (*t*-test, correlated samples).

population from 19% positive in aged control samples to 53% ($P < 0.001$) in AD samples, and in aged control samples, Aβ labeling increased to 87% in LRP1 positives and to 63% ($P < 0.0001$ for each) in LDLR positives. In AD samples, Aβ immunolabeling was increased to 96% in LRP1 positives and to 84% ($P < 0.0001$ for each) in LDLR-positive synaptosomes (Figure 5E). As a negative control, glutamate vesicular transport 1 in the total synaptosome population was quantified, and it was not enriched in either LRP or LDLR positives (data not shown). The Aβ level was higher in LRP1 compared with LDLR receptor positives for both control ($P < 0.001$) and AD synaptosomes ($P < 0.005$) (Figure 5E), likely an indication of the rapid constitutive recycling of LRP1 compared with LDLR receptors.[16] Flow cytometry quantifies both positive fraction and brightness of fluorescence (relative fluorescence units) for each particle in the analysis; fluorescence data for apoE showed elevated apoE levels in LRP1 ($P < 0.03$) compared with LDLR positives ($P < 0.002$) (Figure 5F). Taken together, Figure 5, E and F, is consistent with LRP1 having higher affinity or volume for uptake of apoE/Aβ complex compared with LDLR receptors. Fluorescence data for Aβ (Figure 5G) confirm increased total Aβ in AD compared with control synapses, and also demonstrate markedly higher Aβ in both LRP1-positive ($P < 0.01$) and LDLR-positive ($P < 0.001$) populations compared with control, indicating Aβ localization but not clearance in terminals positive for apoE receptors. These results show that both apoE and Aβ are highly enriched in terminals positive for apoE receptors, with higher levels of both apoE and Aβ colocalized with LRP1 compared with LDLR. More importantly, this colocalization occurs in both AD and control synaptosomes, consistent with apoE and Aβ uptake as a normal, clearance-related function for synaptic apoE receptors. Taken together

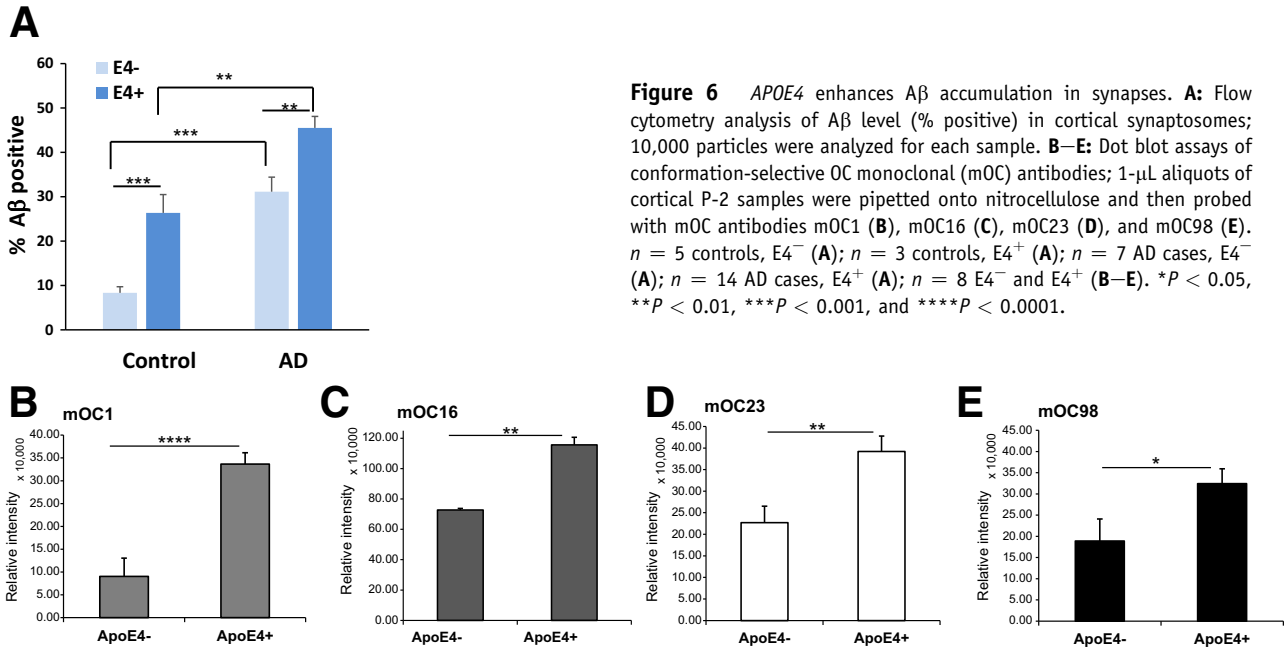

Figure 6 *APOE4* enhances Aβ accumulation in synapses. **A:** Flow cytometry analysis of Aβ level (% positive) in cortical synaptosomes; 10,000 particles were analyzed for each sample. **B**–**E:** Dot blot assays of conformation-selective OC monoclonal (mOC) antibodies; 1-μL aliquots of cortical P-2 samples were pipetted onto nitrocellulose and then probed with mOC antibodies mOC1 (**B**), mOC16 (**C**), mOC23 (**D**), and mOC98 (**E**). $n = 5$ controls, $E4^-$ (**A**); $n = 3$ controls, $E4^+$ (**A**); $n = 7$ AD cases, $E4^-$ (**A**); $n = 14$ AD cases, $E4^+$ (**A**); $n = 8$ $E4^-$ and $E4^+$ (**B**–**E**). $^*P < 0.05$, $^{**}P < 0.01$, $^{***}P < 0.001$, and $^{****}P < 0.0001$.

with the high levels of apoE/Aβ complex in synapses shown above (Figures 1 and 2), these results suggest that apoE/Aβ complex enters synapses via apoE receptors, but the Aβ is cleared only in control (healthy) synapses.

The degree of apoE lipidation is critical for its function; therefore, we next tested the hypothesis that uptake of lipidated apoE/Aβ complex into synapses alters the level of synaptic-free cholesterol and cholesterol esters. Using the same dual-labeling design as above, synaptosomes were labeled for LRP1 and LDLR, along with the lipid dyes filipin (free cholesterol) and Nile red (cholesterol esters). Flow cytometry data were collected from the total population (10,000 particles) and from LDLR- and LRP1-positive synaptosomes (5000 particles/sample), to compare the total synaptic lipid level with the lipid in the receptor-positive synapses. In control synaptosomes, cholesterol esters were increased to approximately the same degree in LRP1 and LDLR positives ($P < 0.01$) (Figure 5H), consistent with receptor-mediated uptake. Cholesterol esters were also elevated in receptor positives in AD; in AD synaptosomes, cholesterol esters were higher in LDLR compared with LRP1 positives ($P < 0.05$). Free cholesterol was increased in LDLR positives in control synaptosomes ($P < 0.05$) (Figure 5I), but was not associated with receptor positives in AD samples, suggesting impaired lipidation of apoE in AD.

APOE4 Enhances Aβ Accumulation in Synapses

APOE4 is well established to increase Aβ deposition in mouse models (E4 > E3 > E2),[5,7,63] human pathology,[64] and imaging studies,[65,66] although the mechanisms are not clear. Given the elevated synaptic Aβ level in AD compared with control cortex in previous results[6,45,46,67] and Figure 5E above, we hypothesized greater Aβ accumulation in E4-containing synaptosomes and quantified Aβ with flow cytometry in aged control and AD cortical synaptosomes. Synaptic Aβ accumulation was higher in both AD groups compared with controls ($P < 0.01$) (Figure 6A) and enhanced in the presence of apoE4 in both control and AD synaptosomes ($P < 0.001$ and $P < 0.01$, respectively) (Figure 6A). Dot blot immunolabeling of P-2 samples with a series of 10 conformation-selective anti-Aβ antibodies[68] revealed E4-mediated increases with four antibodies for fibrillar oligomers (mOC1, $P < 0.0001$; mOC16, $P < 0.01$; mOC23, $P < 0.01$; mOC98, $P < 0.05$) (Figure 6, B–E). Taken together with the results above, uptake of Aβ/apoE complex into AD synaptic terminals results in buildup rather than clearance of Aβ in this neuronal compartment, particularly in the presence of apoE4.

Discussion

APOE has long been implicated in Aβ clearance and Aβ-related toxicity and aggregation, but little clarity exists regarding specific pathways, in particular the existence and possible role of an apoE/Aβ complex and apoE receptors. The present results show increased apoE/Aβ complex in AD cortical synaptosomes and show localization of both LRP1 and LDLR to synaptic terminals. Synaptic LRP1 is up-regulated in AD samples, and the storage form of cholesterol was reduced overall in AD synapses. However, dual-labeling experiments show that apoE and Aβ, along with free and esterified cholesterol, are highly enriched in individual terminals positive for apoE receptors and indicate clearance of Aβ from aged control but not AD synaptosomes. These results have important implications for

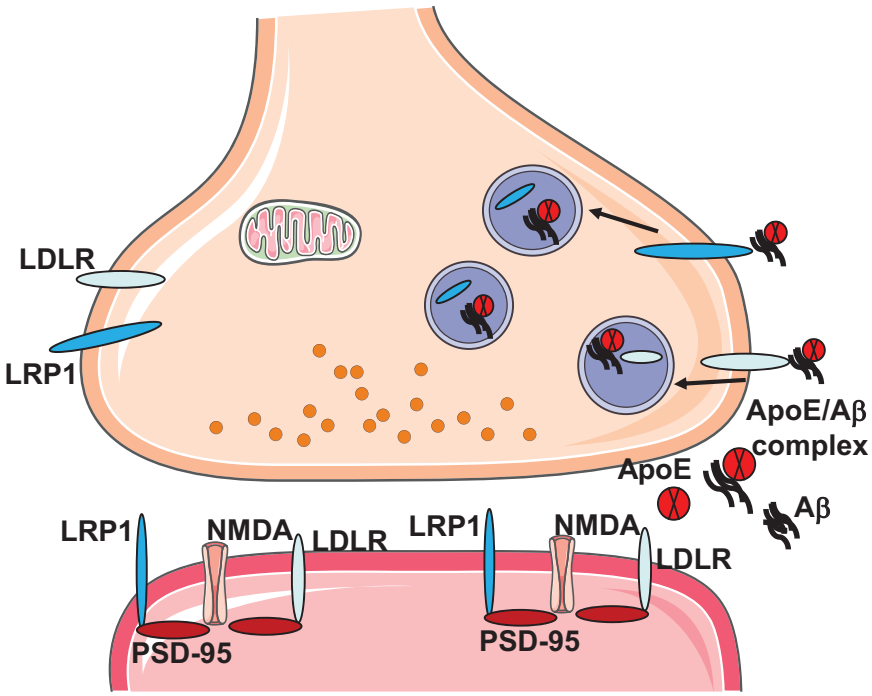

Figure 7 Proposed pathways for apoE and Aβ complex interaction with synaptic apoE receptors. Extracellular apoE/Aβ complex binds to presynaptic LRP1 and LDLR receptors and is internalized into endosomal/autophagic vesicles within the terminal. In synaptic terminals from aged control cortex, apoE/Aβ uptake does not enhance buildup of Aβ. However, complex internalization enhances Aβ accumulation in AD terminals; thus, apoE acts as a pathologic chaperone. Most LRP1 and LDLR are localized to post-synaptic sites, where they colocalize with postsynaptic density-95 (PSD-95) and N-methyl-D-aspartate (NMDA) receptors and mediate multiple signaling functions that include neurite outgrowth, trafficking of glutamate receptors, lipid metabolism, insulin signaling, and antiapoptosis pathways. Post-synaptic signaling complexes may also function in internalization and clearance of Aβ.

pathways related to neuronal clearance versus accumulation of Aβ within the synaptic compartment.

Isoform-dependent complex formation between apoE and Aβ has long been hypothesized as a potential mechanism affecting clearance versus aggregation of Aβ.[36,39] However, the degree to which complex formation occurs in human disease has been controversial (eg, work by Verghese et al[69] found little evidence for complex formation *in vitro* using hypothesized physiological molar ratios of apoE and Aβ). The apoE/Aβ interaction is technically difficult to assess, varying with detection method and specific experimental conditions.[23] ApoE/Aβ complex level also depends on the apoE isoform being studied, its lipidation status, and the cellular compartment generating the apoE,[12,23] which has led to a literature filled with contradictions and inconsistencies. As noted by Kanekiyo et al,[12] the exact apoE and Aβ concentrations and conformations occurring in brain parenchyma are unclear. In the present experiments, the difficulty of modeling conditions is minimized by the use of cryopreserved AD tissue in which membranes and protein concentrations and interactions are preserved.

The marked elevation of apoE/Aβ complex in AD synaptosomes by Western blot analysis, observed in the present results, appears contradictory to our previously published results that soluble apoE/Aβ complex is reduced in AD and by E4 compared with E3.[24] However, sample preparation for the two experiments was different; in the present results, total P-2 pellets were sonicated and the mixture was loaded into lanes. The previous data used a co−enzyme-linked immunosorbent assay to quantify only soluble apoE/Aβ complex in P-2 supernatant after extraction and ultracentrifugation. Therefore, the apoE/Aβ complex in the present results represents total complex, including insoluble complex that was deposited within AD synaptic terminals in endosomes or other membranous structures. Intraterminal deposition would be consistent with previous evidence showing endocytic trafficking of Aβ to lysosomes is a major Aβ clearance pathway,[70] and with evidence that Aβ labeling has been shown to colocalize with cathepsin-D, a marker for acidic organelles, in AD mice expressing human apoE isoforms.[71] Indeed, previous electron microscopy studies document abundant dense Aβ-positive autophagic vesicles in presynaptic terminals and dystrophic neurites.[72−74] Considered together with the present result that apoE/Aβ complex is increased in AD, the previous observation showing reduced soluble complex in AD and in E4 carriers would be expected as a reflection of a sink mechanism, in the same way that cerebral spinal fluid and blood Aβ levels are reduced in AD.

APOE receptors are known to play an important role in internalization of apoE, Aβ, and apoE/Aβ complex, and the important role of *APOE* in Aβ clearance is thought to largely depend on internalization and endocytic trafficking via these receptors.[75,76] Receptors are known to be expressed in neurons, astrocytes, microglia, and endothelial cells[47]; the present results add the synaptic compartment to the list. LRP1-positive synaptosomes have higher levels of apoE and Aβ per terminal compared with LDLR positives, reflecting the known high transport capacity of LRP1.[77] At the same time, apoE and Aβ are highly enriched in both receptor-positive populations, suggesting the operation of both receptors in uptake of these two ligands in the synaptic compartment. Virtually all LRP- and LDLR-positive terminals contain apoE, which may indicate that essentially all

synaptic apoE comes from the extracellular space, most likely from astrocyte processes that envelope the bouton and are necessary for synapse maintenance.[78] On the other hand, Aβ production is primarily neuronal, and Aβ production might occur in the synaptic terminal because inhibition of synaptic activity and endocytosis reduces Aβ production.[79,80] However, the abundance of synaptosomal apoE/Aβ complex and association of Aβ with apoE receptors suggest that, like apoE, much of the synaptic Aβ comes from outside the synapse. LRP interacts with amyloid precursor protein directly and by linkage with the adaptor protein FE65, and is known to promote amyloid precursor protein internalization and Aβ generation.[81–83] This interaction may also underlie the positive association between LRP and synaptic Aβ. However, the striking enrichment of Aβ and apoE in both LRP1- and LDLR-positive synaptosomes and the high levels of apoE/Aβ complex are more consistent with the well-known internalization and clearance functions of both receptors (Figure 7).

An important question with respect to apoE receptors is whether receptor-mediated uptake of Aβ into neurons promotes toxic Aβ accumulation,[16,75] as previously shown.[15,84,85] Our results suggest that apoE and Aβ are internalized as a complex and cleared from control but not AD synapses; LRP1 and LDLR uptake of Aβ into synapses therefore contributes to synaptic Aβ accumulation in AD, with apoE as a pathologic chaperone. Such a model is entirely consistent with evidence that Aβ deposition is reduced by antibodies that block apoE[26,27] or the apoE/Aβ interaction,[86–90] and suggests the apoE/Aβ complex as a potential therapeutic target.

Both LDLR and LRP1 are known to colocalize with N-methyl-D-aspartate receptor and other post-synaptic proteins, and to possess signaling as well as endocytic functions.[50–52] For example, binding of tissue-type plasminogen activator or α2 macroglobulin to LRP1 transactivates tropomyosin receptor kinase receptor via Src family kinase, resulting in neurite outgrowth, along with regulation of cellular calcium levels via N-methyl-D-aspartate receptors.[57] The present results confirm previous observations of post-synaptic localization,[16,53] and also indicate that a population of apoE receptors is presynaptic. Some studies suggest that LRP1 signaling and endocytic functions are independent of each other.[91] Therefore, taken together with our previous data showing apoE and Aβ colocalization in synaptosomes,[6] the present data seem most consistent with a neuronal model in which a separate population of receptors on the presynaptic terminal mediates uptake of apoE and Aβ into the lysosomal pathway, with post-synaptic receptors mediating various signaling pathways. However, it may be possible for LRP1 signaling complexes interacting with the post-synaptic scaffold to also function in endocytosis and clearance of Aβ, and the present experiments do not examine the localization of downstream pathways or different cell types, such as astrocytes.

A primary function of brain apoE is delivery of lipids, vital for synaptic maintenance and repair,[92,93] to neurons via apoE receptors.[12] For example, deletion of the apoE receptor LRP1 results in global lipid deficits along with spine degeneration and synapse loss.[94] Free cholesterol is loaded onto apoE by the ATP-binding cassette transporter (ABCA1), and as the high-density lipoprotein particles mature, they become spherical with a cholesterol ester core. In the present work, control synaptosomes positive for apoE receptors demonstrated a measurable increase in synaptic cholesterol and cholesterol esters, consistent with uptake of an apoE/Aβ complex along with its associated lipids. In receptor-positive AD synaptosomes, apoE and Aβ accumulation was not accompanied by increased cholesterol, possibly indicating uptake of poorly lipidated apoE. A relative lack of cholesterol in AD synapses might also be a sign of altered membrane fluidity[95] and Aβ-induced synaptic dysfunction. The elevated cholesterol esters in LDLR positives in AD may indicate an LDLR-mediated compensatory up-regulation in cholesterol stores that only operates in relatively healthy control synapses. The lipid alterations observed herein are consistent with *in vitro* experiments showing similar apoE-dependent cholesterol uptake in both neurons and astrocytes.[96]

Notably, evidence suggests that the cellular distribution of cholesterol is likely to be more important than the total cholesterol level, and a delicate balance between membrane-free cholesterol and cholesterol esters is regulated by the enzyme that catalyzes CE formation, acyl—coenzyme A/cholesterol acyltransferase (ACT).[97] The CE storage form exists as lipid droplets and represents approximately 1% of the total[98]; the present results show a reduction in CE across disease stage, consistent with work showing that Aβ reduces cholesterol esterification.[99] Our findings are also in strong agreement with previous work showing age-related memory deficits are induced when cholesterol esters are reduced and free cholesterol is increased[100]; these authors suggest that Aβ fibrils may bind to free cholesterol in the membrane and attenuate the conversion of free to esterified cholesterol. On the other hand, cholesterol esters were increased in a lipidomic study of AD entorhinal cortex and three mouse models,[101] highlighting the need for further study of cholesterol distribution in specific compartments.

A complete understanding of the function and nature of the apoE/Aβ complex is critical for improving AD therapies, and it has relevance for multiple neurodegenerative conditions. The present work used flow cytometry analysis and cryopreserved AD samples to quantify apoE receptors in the synaptic compartment and to examine associations between apoE and its receptors, and with Aβ and lipid levels. Our findings are consistent with a hypothesis that apoE/Aβ complex is transported into synaptic terminals via apoE receptors and demonstrate the feasibility of accurately measuring lipid levels in this compartment, making it possible to examine other apoE receptors in future experiments. The apoE receptors LRP1 and LDLR may enhance

Aβ clearance in other cell types, such as astrocytes and endothelial cells, but the present results suggest that apoE receptors enhance Aβ accumulation in the neuronal synaptic compartment in AD, an internalization role with important implications for LRP1 and LDLR as therapeutic strategies.

References

1. Dickson TC, Saunders HL, Vickers JC: Relationship between apolipoprotein E and the amyloid deposits and dystrophic neurites of Alzheimer's disease. Neuropathol Appl Neurobiol 1997, 23:483−491
2. Burns MP, Noble WJ, Olm V, Gaynor K, Casey E, LaFrancois J, Wang L, Duff K: Co-localization of cholesterol, apolipoprotein E and fibrillar Abeta in amyloid plaques. Brain Res Mol Brain Res 2003, 110:119−125
3. Yu JT, Tan L, Hardy J: Apolipoprotein E in Alzheimer's disease: an update. Annu Rev Neurosci 2014, 37:79−100
4. Mori T, Paris D, Town T, Rojiani AM, Sparks DL, Delledonne A, Crawford F, Abdullah LI, Humphrey JA, Dickson DW, Mullan MJ: Cholesterol accumulates in senile plaques of Alzheimer disease patients and in transgenic APP(SW) mice. J Neuropathol Exp Neurol 2001, 60:778−785
5. Bales KR, Liu F, Wu S, Lin S, Koger D, DeLong C, Hansen JC, Sullivan PM, Paul SM: Human APOE isoform-dependent effects on brain beta-amyloid levels in PDAPP transgenic mice. J Neurosci 2009, 29:6771−6779
6. Arold S, Sullivan P, Bilousova T, Teng E, Miller CA, Poon WW, Vinters HV, Cornwell LB, Saing T, Cole GM, Gylys KH: Apolipoprotein E level and cholesterol are associated with reduced synaptic amyloid beta in Alzheimer's disease and apoE TR mouse cortex. Acta Neuropathol 2012, 123:39−52
7. Castellano JM, Kim J, Stewart FR, Jiang H, Demattos RB, Patterson BW, Fagan AM, Morris JC, Mawuenyega KG, Cruchaga C, Goate AM, Bales KR, Paul SM, Bateman RJ, Holtzman DM: Human apoE isoforms differentially regulate brain amyloid-{beta} peptide clearance. Sci Transl Med 2011, 3:89ra57
8. Jiang Q, Lee CY, Mandrekar S, Wilkinson B, Cramer P, Zelcer N, Mann K, Lamb B, Willson TM, Collins JL, Richardson JC, Smith JD, Comery TA, Riddell D, Holtzman DM, Tontonoz P, Landreth GE: ApoE promotes the proteolytic degradation of Abeta. Neuron 2008, 58:681−693
9. Deane R, Sagare A, Hamm K, Parisi M, Lane S, Finn MB, Holtzman DM, Zlokovic BV: apoE isoform-specific disruption of amyloid beta peptide clearance from mouse brain. J Clin Invest 2008, 118:4002−4013
10. Bell RD, Sagare AP, Friedman AE, Bedi GS, Holtzman DM, Deane R, Zlokovic BV: Transport pathways for clearance of human Alzheimer's amyloid beta-peptide and apolipoproteins E and J in the mouse central nervous system. J Cereb Blood Flow Metab 2007, 27:909−918
11. DeMattos RB, Cirrito JR, Parsadanian M, May PC, O'Dell MA, Taylor JW, Harmony JA, Aronow BJ, Bales KR, Paul SM, Holtzman DM: ApoE and clusterin cooperatively suppress Abeta levels and deposition: evidence that ApoE regulates extracellular Abeta metabolism in vivo. Neuron 2004, 41:193−202
12. Kanekiyo T, Xu H, Bu G: ApoE and Abeta in Alzheimer's disease: accidental encounters or partners? Neuron 2014, 81:740−754
13. Kim J, Castellano JM, Jiang H, Basak JM, Parsadanian M, Pham V, Mason SM, Paul SM, Holtzman DM: Overexpression of low-density lipoprotein receptor in the brain markedly inhibits amyloid deposition and increases extracellular A beta clearance. Neuron 2009, 64:632−644
14. Kanekiyo T, Cirrito JR, Liu CC, Shinohara M, Li J, Schuler DR, Shinohara M, Holtzman DM, Bu G: Neuronal clearance of amyloid-beta by endocytic receptor LRP1. J Neurosci 2013, 33:19276−19283
15. Billings LM, Oddo S, Green KN, McGaugh JL, LaFerla FM: Intraneuronal Abeta causes the onset of early Alzheimer's disease-related cognitive deficits in transgenic mice. Neuron 2005, 45:675−688
16. Shinohara M, Tachibana M, Kanekiyo T, Bu G: Role of LRP1 in the pathogenesis of Alzheimer's disease: evidence from clinical and preclinical studies. J Lipid Res 2017, 58:1267−1281
17. Mandrekar S, Jiang Q, Lee CY, Koenigsknecht-Talboo J, Holtzman DM, Landreth GE: Microglia mediate the clearance of soluble Abeta through fluid phase macropinocytosis. J Neurosci 2009, 29:4252−4262
18. Koistinaho M, Lin S, Wu X, Esterman M, Koger D, Hanson J, Higgs R, Liu F, Malkani S, Bales KR, Paul SM: Apolipoprotein E promotes astrocyte colocalization and degradation of deposited amyloid-beta peptides. Nat Med 2004, 10:719−726
19. Holtzman DM, Herz J, Bu G: Apolipoprotein E and apolipoprotein E receptors: normal biology and roles in Alzheimer disease. Cold Spring Harb Perspect Med 2012, 2:a006312
20. Russo C, Angelini G, Dapino D, Piccini A, Piombo G, Schettini G, Chen S, Teller JK, Zaccheo D, Gambetti P, Tabaton M: Opposite roles of apolipoprotein E in normal brains and in Alzheimer's disease. Proc Natl Acad Sci U S A 1998, 95:15598−15602
21. Koudinov AR, Berezov TT, Kumar A, Koudinova NV: Alzheimer's amyloid beta interaction with normal human plasma high density lipoprotein: association with apolipoprotein and lipids. Clin Chim Acta 1998, 270:75−84
22. LaDu MJ, Munson GW, Jungbauer L, Getz GS, Reardon CA, Tai LM, Yu C: Preferential interactions between ApoE-containing lipoproteins and Abeta revealed by a detection method that combines size exclusion chromatography with non-reducing gel-shift. Biochim Biophys Acta 2012, 1821:295−302
23. Tai LM, Mehra S, Shete V, Estus S, Rebeck GW, Bu G, LaDu MJ: Soluble apoE/Abeta complex: mechanism and therapeutic target for APOE4-induced AD risk. Mol Neurodegener 2014, 9:2
24. Tai LM, Bilousova T, Jungbauer L, Roeske SK, Youmans KL, Yu C, Poon WW, Cornwell LB, Miller CA, Vinters HV, Van Eldik LJ, Fardo DW, Estus S, Bu G, Gylys KH, Ladu MJ: Levels of soluble apolipoprotein E/amyloid-beta complex are reduced and oligomeric Abeta increased with APOE4 and Alzheimer disease in a transgenic mouse model and human samples. J Biol Chem 2013, 288:5914−5926
25. Hu J, Liu CC, Chen XF, Zhang YW, Xu H, Bu G: Opposing effects of viral mediated brain expression of apolipoprotein E2 (apoE2) and apoE4 on apoE lipidation and Abeta metabolism in apoE4-targeted replacement mice. Mol Neurodegener 2015, 10:6
26. Kim J, Eltorai AE, Jiang H, Liao F, Verghese PB, Kim J, Stewart FR, Basak JM, Holtzman DM: Anti-apoE immunotherapy inhibits amyloid accumulation in a transgenic mouse model of Abeta amyloidosis. J Exp Med 2012, 209:2149−2156
27. Liao F, Hori Y, Hudry E, Bauer AQ, Jiang H, Mahan TE, Lefton KB, Zhang TJ, Dearborn JT, Kim J, Culver JP, Betensky R, Wozniak DF, Hyman BT, Holtzman DM: Anti-ApoE antibody given after plaque onset decreases Abeta accumulation and improves brain function in a mouse model of Abeta amyloidosis. J Neurosci 2014, 34:7281−7292
28. Liu S, Breitbart A, Sun Y, Mehta PD, Boutajangout A, Scholtzova H, Wisniewski T: Blocking the apolipoprotein E/amyloid beta interaction in triple transgenic mice ameliorates Alzheimer's disease related amyloid beta and tau pathology. J Neurochem 2014, 128:577−591
29. Gylys KH, Fein JA, Tan AM, Cole GM: Apolipoprotein E enhances uptake of soluble but not aggregated amyloid-beta protein into synaptic terminals. J Neurochem 2003, 84:1442−1451

30. Yang F, Mak K, Vinters HV, Frautschy SA, Cole GM: Monoclonal antibody to the C-terminus of beta-amyloid. Neuroreport 1994, 5: 2117–2120
31. Hatami A, Albay R 3rd, Monjazeb S, Milton S, Glabe C: Monoclonal antibodies against Abeta42 fibrils distinguish multiple aggregation state polymorphisms in vitro and in Alzheimer disease brain. J Biol Chem 2014, 289:32131–32143
32. Bilousova T, Miller CA, Poon WW, Vinters HV, Corrada M, Kawas C, Hayden EY, Teplow DB, Glabe C, Albay R 3rd, Cole GM, Teng E, Gylys KH: Synaptic amyloid-beta oligomers precede p-tau and differentiate high pathology control cases. Am J Pathol 2016, 186:185–198
33. Dodd PR, Hardy JA, Baig EB, Kidd AM, Bird ED, Watson WE, Johnston GA: Optimization of freezing, storage, and thawing conditions for the preparation of metabolically active synaptosomes from frozen rat and human brain. Neurochem Pathol 1986, 4:177–198
34. Pang J, Wu Y, Peng J, Yang P, Kuai L, Qin X, Cao F, Sun X, Chen L, Vitek MP, Jiang Y: Potential implications of apolipoprotein E in early brain injury after experimental subarachnoid hemorrhage: involvement in the modulation of blood-brain barrier integrity. Oncotarget 2016, 7:56030–56044
35. Gylys KH, Fein JA, Yang F, Cole GM: Enrichment of presynaptic and postsynaptic markers by size-based gating analysis of synaptosome preparations from rat and human cortex. Cytometry A 2004, 60: 90–96
36. LaDu MJ, Lukens JR, Reardon CA, Getz GS: Association of human, rat, and rabbit apolipoprotein E with beta-amyloid. J Neurosci Res 1997, 49:9–18
37. Munson GW, Roher AE, Kuo YM, Gilligan SM, Reardon CA, Getz GS, LaDu MJ: SDS-stable complex formation between native apolipoprotein E3 and beta-amyloid peptides. Biochemistry 2000, 39: 16119–16124
38. Chan W, Fornwald J, Brawner M, Wetzel R: Native complex formation between apolipoprotein E isoforms and the Alzheimer's disease peptide A beta. Biochemistry 1996, 35:7123–7130
39. LaDu MJ, Falduto MT, Manelli AM, Reardon CA, Getz GS, Frail DE: Isoform-specific binding of apolipoprotein E to beta-amyloid. J Biol Chem 1994, 269:23403–23406
40. Golabek AA, Soto C, Vogel T, Wisniewski T: The interaction between apolipoprotein E and Alzheimer's amyloid beta-peptide is dependent on beta-peptide conformation. J Biol Chem 1996, 271: 10602–10606
41. Morikawa M, Fryer JD, Sullivan PM, Christopher EA, Wahrle SE, DeMattos RB, O'Dell MA, Fagan AM, Lashuel HA, Walz T, Asai K, Holtzman DM: Production and characterization of astrocyte-derived human apolipoprotein E isoforms from immortalized astrocytes and their interactions with amyloid-beta. Neurobiol Dis 2005, 19:66–76
42. Lesne S, Kotilinek L, Ashe KH: Plaque-bearing mice with reduced levels of oligomeric amyloid-beta assemblies have intact memory function. Neuroscience 2008, 151:745–749
43. Lesne SE, Sherman MA, Grant M, Kuskowski M, Schneider JA, Bennett DA, Ashe KH: Brain amyloid-beta oligomers in ageing and Alzheimer's disease. Brain 2013, 136:1383–1398
44. Roychaudhuri R, Zheng X, Lomakin A, Maiti P, Condron MM, Benedek GB, Bitan G, Bowers MT, Teplow DB: Role of species-specific primary structure differences in Abeta42 assembly and neurotoxicity. ACS Chem Neurosci 2015, 6:1941–1955
45. Sokolow S, Henkins KM, Bilousova T, Miller CA, Vinters HV, Poon W, Cole GM, Gylys KH: AD synapses contain abundant Abeta monomer and multiple soluble oligomers, including a 56-kDa assembly. Neurobiol Aging 2012, 33:1545–1555
46. Fein JA, Sokolow S, Miller CA, Vinters HV, Yang F, Cole GM, Gylys KH: Co-localization of amyloid beta and tau pathology in Alzheimer's disease synaptosomes. Am J Pathol 2008, 172: 1683–1692
47. Kanekiyo T, Bu G: The low-density lipoprotein receptor-related protein 1 and amyloid-beta clearance in Alzheimer's disease. Front Aging Neurosci 2014, 6:93
48. Kanekiyo T, Zhang J, Liu Q, Liu CC, Zhang L, Bu G: Heparan sulphate proteoglycan and the low-density lipoprotein receptor-related protein 1 constitute major pathways for neuronal amyloid-beta uptake. J Neurosci 2011, 31:1644–1651
49. Zlokovic BV, Deane R, Sagare AP, Bell RD, Winkler EA: Low-density lipoprotein receptor-related protein-1: a serial clearance homeostatic mechanism controlling Alzheimer's amyloid beta-peptide elimination from the brain. J Neurochem 2010, 115: 1077–1089
50. Maier W, Bednorz M, Meister S, Roebroek A, Weggen S, Schmitt U, Pietrzik CU: LRP1 is critical for the surface distribution and internalization of the NR2B NMDA receptor subtype. Mol Neurodegener 2013, 8:25
51. Rebeck GW: Nontraditional signaling mechanisms of lipoprotein receptors. Sci Signal 2009, 2:pe28
52. May P, Rohlmann A, Bock HH, Zurhove K, Marth JD, Schomburg ED, Noebels JL, Beffert U, Sweatt JD, Weeber EJ, Herz J: Neuronal LRP1 functionally associates with postsynaptic proteins and is required for normal motor function in mice. Mol Cell Biol 2004, 24:8872–8883
53. Gotthardt M, Trommsdorff M, Nevitt MF, Shelton J, Richardson JA, Stockinger W, Nimpf J, Herz J: Interactions of the low density lipoprotein receptor gene family with cytosolic adaptor and scaffold proteins suggest diverse biological functions in cellular communication and signal transduction. J Biol Chem 2000, 275:25616–25624
54. Stockinger W, Hengstschlager-Ottnad E, Novak S, Matus A, Huttinger M, Bauer J, Lassmann H, Schneider WJ, Nimpf J: The low density lipoprotein receptor gene family: differential expression of two alpha2-macroglobulin receptors in the brain. J Biol Chem 1998, 273:32213–32221
55. Sokolow S, Henkins KM, Williams IA, Vinters HV, Schmid I, Cole GM, Gylys KH: Isolation of synaptic terminals from Alzheimer's disease cortex. Cytometry A 2012, 81:248–254
56. Sokolow S, Luu SH, Nandy K, Miller CA, Vinters HV, Poon WW, Gylys KH: Preferential accumulation of amyloid-beta in presynaptic glutamatergic terminals (VGluT1 and VGluT2) in Alzheimer's disease cortex. Neurobiol Dis 2012, 45:381–387
57. Shi Y, Mantuano E, Inoue G, Campana WM, Gonias SL: Ligand binding to LRP1 transactivates Trk receptors by a Src family kinase-dependent pathway. Sci Signal 2009, 2:ra18
58. Bacskai BJ, Xia MQ, Strickland DK, Rebeck GW, Hyman BT: The endocytic receptor protein LRP also mediates neuronal calcium signaling via N-methyl-D-aspartate receptors. Proc Natl Acad Sci U S A 2000, 97:11551–11556
59. Sato N, Morishita R: The roles of lipid and glucose metabolism in modulation of beta-amyloid, tau, and neurodegeneration in the pathogenesis of Alzheimer disease. Front Aging Neurosci 2015, 7:199
60. Muller CP, Stephany DA, Winkler DF, Hoeg JM, Demosky SJ Jr, Wunderlich JR: Filipin as a flow microfluorometry probe for cellular cholesterol. Cytometry 1984, 5:42–54
61. Gylys KH, Fein JA, Yang F, Miller CA, Cole GM: Increased cholesterol in Abeta-positive nerve terminals from Alzheimer's disease cortex. Neurobiol Aging 2007, 28:8–17
62. Pani A, Dessi S, Diaz G, La Colla P, Abete C, Mulas C, Angius F, Cannas MD, Orru CD, Cocco PL, Mandas A, Putzu P, Laurenzana A, Cellai C, Costanza AM, Bavazzano A, Mocali A, Paoletti F: Altered cholesterol ester cycle in skin fibroblasts from patients with Alzheimer's disease. J Alzheimers Dis 2009, 18:829–841
63. Youmans KL, Tai LM, Nwabuisi-Heath E, Jungbauer L, Kanekiyo T, Gan M, Kim J, Eimer WA, Estus S, Rebeck GW, Weeber EJ, Bu G, Yu C, Ladu MJ: APOE4-specific changes in Abeta accumulation in a new transgenic mouse model of Alzheimer disease. J Biol Chem 2012, 287:41774–41786

64. Christensen DZ, Schneider-Axmann T, Lucassen PJ, Bayer TA, Wirths O: Accumulation of intraneuronal Abeta correlates with ApoE4 genotype. Acta Neuropathol 2010, 119:555–566
65. Reiman EM, Chen K, Liu X, Bandy D, Yu M, Lee W, Ayutyanont N, Keppler J, Reeder SA, Langbaum JB, Alexander GE, Klunk WE, Mathis CA, Price JC, Aizenstein HJ, DeKosky ST, Caselli RJ: Fibrillar amyloid-beta burden in cognitively normal people at 3 levels of genetic risk for Alzheimer's disease. Proc Natl Acad Sci U S A 2009, 106:6820–6825
66. Morris JC, Roe CM, Xiong C, Fagan AM, Goate AM, Holtzman DM, Mintun MA: APOE predicts amyloid-beta but not tau Alzheimer pathology in cognitively normal aging. Ann Neurol 2010, 67: 122–131
67. Gylys KH, Fein JA, Yang F, Wiley DJ, Miller CA, Cole GM: Synaptic changes in Alzheimer's disease: increased amyloid-beta and gliosis in surviving terminals is accompanied by decreased PSD-95 fluorescence. Am J Pathol 2004, 165:1809–1817
68. Hatami A, Monjazeb S, Milton S, Glabe CG: Familial Alzheimer's disease mutations within the amyloid precursor protein alter the aggregation and conformation of the amyloid-beta peptide. J Biol Chem 2017, 292:3172–3185
69. Verghese PB, Castellano JM, Garai K, Wang Y, Jiang H, Shah A, Bu G, Frieden C, Holtzman DM: ApoE influences amyloid-beta (Abeta) clearance despite minimal apoE/Abeta association in physiological conditions. Proc Natl Acad Sci U S A 2013, 110: E1807–E1816
70. Li J, Kanekiyo T, Shinohara M, Zhang Y, LaDu MJ, Xu H, Bu G: Differential regulation of amyloid-beta endocytic trafficking and lysosomal degradation by apolipoprotein E isoforms. J Biol Chem 2012, 287:44593–44601
71. Youmans KL, Tai LM, Kanekiyo T, Stine WB Jr, Michon SC, Nwabuisi-Heath E, Manelli AM, Fu Y, Riordan S, Eimer WA, Binder L, Bu G, Yu C, Hartley DM, LaDu MJ: Intraneuronal Abeta detection in 5xFAD mice by a new Abeta-specific antibody. Mol Neurodegener 2012, 7:8
72. Takahashi RH, Milner TA, Li F, Nam EE, Edgar MA, Yamaguchi H, Beal MF, Xu H, Greengard P, Gouras GK: Intraneuronal Alzheimer abeta42 accumulates in multivesicular bodies and is associated with synaptic pathology. Am J Pathol 2002, 161:1869–1879
73. Nixon RA, Wegiel J, Kumar A, Yu WH, Peterhoff C, Cataldo A, Cuervo AM: Extensive involvement of autophagy in Alzheimer disease: an immuno-electron microscopy study. J Neuropathol Exp Neurol 2005, 64:113–122
74. Sanchez-Varo R, Trujillo-Estrada L, Sanchez-Mejias E, Torres M, Baglietto-Vargas D, Moreno-Gonzalez I, De Castro V, Jimenez S, Ruano D, Vizuete M, Davila JC, Garcia-Verdugo JM, Jimenez AJ, Vitorica J, Gutierrez A: Abnormal accumulation of autophagic vesicles correlates with axonal and synaptic pathology in young Alzheimer's mice hippocampus. Acta Neuropathol 2012, 123:53–70
75. Bu G: Apolipoprotein E and its receptors in Alzheimer's disease: pathways, pathogenesis and therapy. Nat Rev Neurosci 2009, 10: 333–344
76. Lane-Donovan C, Philips GT, Herz J: More than cholesterol transporters: lipoprotein receptors in CNS function and neurodegeneration. Neuron 2014, 83:771–787
77. Li Y, Lu W, Marzolo MP, Bu G: Differential functions of members of the low density lipoprotein receptor family suggested by their distinct endocytosis rates. J Biol Chem 2001, 276:18000–18006
78. Ullian EM, Sapperstein SK, Christopherson KS, Barres BA: Control of synapse number by glia. Science 2001, 291:657–661
79. Cirrito JR, Kang JE, Lee J, Stewart FR, Verges DK, Silverio LM, Bu G, Mennerick S, Holtzman DM: Endocytosis is required for synaptic activity-dependent release of amyloid-beta in vivo. Neuron 2008, 58:42–51
80. Cirrito JR, Yamada KA, Finn MB, Sloviter RS, Bales KR, May PC, Schoepp DD, Paul SM, Mennerick S, Holtzman DM: Synaptic activity regulates interstitial fluid amyloid-beta levels in vivo. Neuron 2005, 48:913–922
81. Waldron E, Heilig C, Schweitzer A, Nadella N, Jaeger S, Martin AM, Weggen S, Brix K, Pietrzik CU: LRP1 modulates APP trafficking along early compartments of the secretory pathway. Neurobiol Dis 2008, 31:188–197
82. Pietrzik CU, Yoon IS, Jaeger S, Busse T, Weggen S, Koo EH: FE65 constitutes the functional link between the low-density lipoprotein receptor-related protein and the amyloid precursor protein. J Neurosci 2004, 24:4259–4265
83. Pietrzik CU, Busse T, Merriam DE, Weggen S, Koo EH: The cytoplasmic domain of the LDL receptor-related protein regulates multiple steps in APP processing. EMBO J 2002, 21:5691–5700
84. Wilhelmus MM, Otte-Holler I, van Triel JJ, Veerhuis R, Maat-Schieman ML, Bu G, de Waal RM, Verbeek MM: Lipoprotein receptor-related protein-1 mediates amyloid-beta-mediated cell death of cerebrovascular cells. Am J Pathol 2007, 171:1989–1999
85. Rushworth JV, Griffiths HH, Watt NT, Hooper NM: Prion protein-mediated toxicity of amyloid-beta oligomers requires lipid rafts and the transmembrane LRP1. J Biol Chem 2013, 288:8935–8951
86. Pankiewicz JE, Guridi M, Kim J, Asuni AA, Sanchez S, Sullivan PM, Holtzman DM, Sadowski MJ: Blocking the apoE/Abeta interaction ameliorates Abeta-related pathology in APOE epsilon2 and epsilon4 targeted replacement Alzheimer model mice. Acta Neuropathol Commun 2014, 2:75
87. Hao J, Zhang W, Zhang P, Liu R, Liu L, Lei G, Su C, Miao J, Li Z: Abeta20-29 peptide blocking apoE/Abeta interaction reduces full-length Abeta42/40 fibril formation and cytotoxicity in vitro. Neuropeptides 2010, 44:305–313
88. Kuszczyk MA, Sanchez S, Pankiewicz J, Kim J, Duszczyk M, Guridi M, Asuni AA, Sullivan PM, Holtzman DM, Sadowski MJ: Blocking the interaction between apolipoprotein E and Abeta reduces intraneuronal accumulation of Abeta and inhibits synaptic degeneration. Am J Pathol 2013, 182:1750–1768
89. Sadowski M, Pankiewicz J, Scholtzova H, Ripellino JA, Li Y, Schmidt SD, Mathews PM, Fryer JD, Holtzman DM, Sigurdsson EM, Wisniewski T: A synthetic peptide blocking the apolipoprotein E/beta-amyloid binding mitigates beta-amyloid toxicity and fibril formation in vitro and reduces beta-amyloid plaques in transgenic mice. Am J Pathol 2004, 165:937–948
90. Sadowski MJ, Pankiewicz J, Scholtzova H, Mehta PD, Prelli F, Quartermain D, Wisniewski T: Blocking the apolipoprotein E/amyloid-beta interaction as a potential therapeutic approach for Alzheimer's disease. Proc Natl Acad Sci U S A 2006, 103:18787–18792
91. Lillis AP, Van Duyn LB, Murphy-Ullrich JE, Strickland DK: LDL receptor-related protein 1: unique tissue-specific functions revealed by selective gene knockout studies. Physiol Rev 2008, 88:887–918
92. Mauch DH, Nagler K, Schumacher S, Goritz C, Muller EC, Otto A, Pfrieger FW: CNS synaptogenesis promoted by glia-derived cholesterol. Science 2001, 294:1354–1357
93. Hering H, Lin CC, Sheng M: Lipid rafts in the maintenance of synapses, dendritic spines, and surface AMPA receptor stability. J Neurosci 2003, 23:3262–3271
94. Liu Q, Trotter J, Zhang J, Peters MM, Cheng H, Bao J, Han X, Weeber EJ, Bu G: Neuronal LRP1 knockout in adult mice leads to impaired brain lipid metabolism and progressive, age-dependent synapse loss and neurodegeneration. J Neurosci 2010, 30: 17068–17078
95. Wood WG, Schroeder F, Igbavboa U, Avdulov NA, Chochina SV: Brain membrane cholesterol domains, aging and amyloid beta-peptides. Neurobiol Aging 2002, 23:685–694
96. Rapp A, Gmeiner B, Huttinger M: Implication of apoE isoforms in cholesterol metabolism by primary rat hippocampal neurons and astrocytes. Biochimie 2006, 88:473–483
97. Puglielli L, Konopka G, Pack-Chung E, Ingano LA, Berezovska O, Hyman BT, Chang TY, Tanzi RE, Kovacs DM: Acyl-coenzyme A:

cholesterol acyltransferase modulates the generation of the amyloid beta-peptide. Nat Cell Biol 2001, 3:905−912

98. Petrov AM, Kasimov MR, Zefirov AL: Brain cholesterol metabolism and its defects: linkage to neurodegenerative diseases and synaptic dysfunction. Acta Naturae 2016, 8:58−73
99. Marquer C, Laine J, Dauphinot L, Hanbouch L, Lemercier-Neuillet C, Pierrot N, Bossers K, Le M, Corlier F, Benstaali C, Saudou F, Thinakaran G, Cartier N, Octave JN, Duyckaerts C, Potier MC: Increasing membrane cholesterol of neurons in culture recapitulates Alzheimer's disease early phenotypes. Mol Neurodegener 2014, 9:60
100. Liu Y, Peterson DA, Schubert D: Amyloid beta peptide alters intracellular vesicle trafficking and cholesterol homeostasis. Proc Natl Acad Sci U S A 1998, 95:13266−13271
101. Chan RB, Oliveira TG, Cortes EP, Honig LS, Duff KE, Small SA, Wenk MR, Shui G, Di Paolo G: Comparative lipidomic analysis of mouse and human brain with Alzheimer disease. J Biol Chem 2012, 287:2678−2688